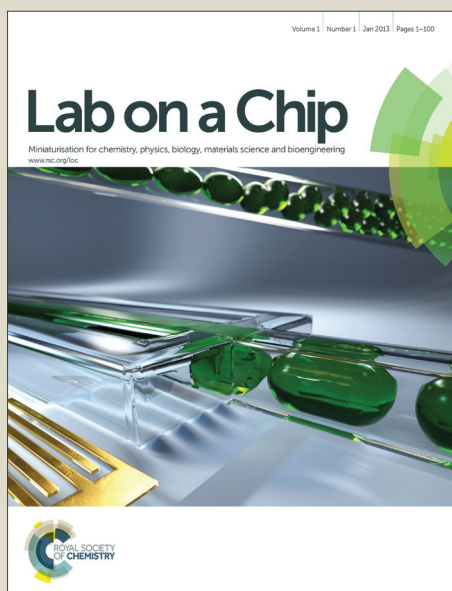


Lab on a Chip

Accepted Manuscript



This article can be cited before page numbers have been issued, to do this please use: M. Erickstad, E. Gutierrez and A. Groisman, *Lab Chip*, 2014, DOI: 10.1039/C4LC00472H.



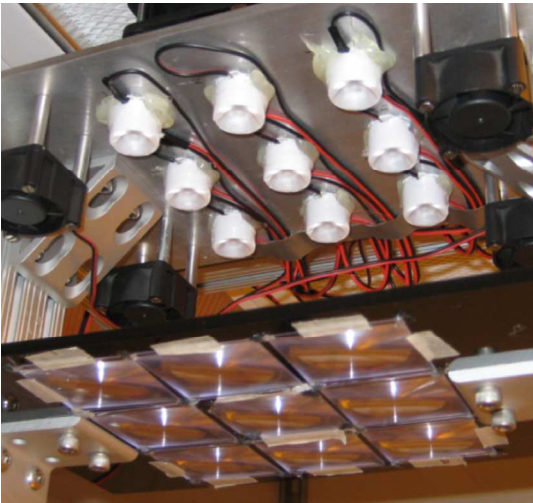
This is an *Accepted Manuscript*, which has been through the Royal Society of Chemistry peer review process and has been accepted for publication.

Accepted Manuscripts are published online shortly after acceptance, before technical editing, formatting and proof reading. Using this free service, authors can make their results available to the community, in citable form, before we publish the edited article. We will replace this *Accepted Manuscript* with the edited and formatted *Advance Article* as soon as it is available.

You can find more information about *Accepted Manuscripts* in the [Information for Authors](#).

Please note that technical editing may introduce minor changes to the text and/or graphics, which may alter content. The journal's standard [Terms & Conditions](#) and the [Ethical guidelines](#) still apply. In no event shall the Royal Society of Chemistry be held responsible for any errors or omissions in this *Accepted Manuscript* or any consequences arising from the use of any information it contains.

An LED-based UV-light source producing collimated uniform illumination over a large area is built and used to fabricate PDMS microchannels with near-rectangular profiles and depths up to 300 μm .



TECHNICAL INNOVATION

A low-cost low-maintenance ultraviolet lithography light source based on light-emitting diodes

Cite this: DOI: 10.1039/C4LC00472H

M. Erickstad,^a E. Gutierrez^a and A. Groisman^{a,*}Received 10th January 2012,
Accepted 10th January 2012

DOI: 10.1039/C4LC00472H

www.rsc.org/

A source of collimated ultraviolet (UV) light is a central piece of equipment needed for lithographic fabrication of microfluidic devices. Conventional UV light sources based on high-pressure mercury lamps require considerable maintenance and provide broad-band illumination with intensity that often changes with time. Here we present a source of narrow-band UV light based on an array of nine 365 nm light-emitting diodes (LEDs). Each LED has two dedicated converging lenses, reducing the divergence of light emanating from it to 5.4°. Partial overlap of the areas illuminated by individual LEDs provides UV illumination with a mean intensity of $\sim 1.7 \text{ mW/cm}^2$ and coefficient of variation $< 3\%$ over a $90 \times 90 \text{ mm}$ target area. The light source was used to lithographically fabricate micro-reliefs with thicknesses from ~ 25 to $311 \text{ }\mu\text{m}$ with SU8 photoresists. A cumulative irradiation of 370 mJ/cm^2 (4 min exposure) produced reliefs of good quality for all SU8 thicknesses. Polydimethylsiloxane (PDMS) replicas of the SU8 reliefs had microchannels with nearly rectangular cross-sections that were highly consistent over the entire target area, and partitions between the channels had depth to width ratios up to 5. The UV light source has also been successfully used for photolithography with positive photoresists, AZ40XT and SPR-220. The proposed light source is built with a total cost of $< \$1000$, consumes a minimal amount of power, is expected to last for $\sim 50,000$ exposures, maintenance-free, and is particularly appealing for small research-and-development microfluidic fabrication.

Introduction

Microfluidic devices made of silicone rubber are widely used in the research community. Master molds for these devices can be rapidly fabricated by using photolithography to form various reliefs of photoresist on silicon wafers. This process of rapid prototyping is particularly appealing, because it does not require much space and equipment. A common choice of photoresist for rapid prototyping is one of the ultraviolet (UV)-curable epoxies from the SU8 family. The SU8 epoxies enable the fabrication of microchannels with a broad range of thickness, from < 1 to $> 500 \text{ }\mu\text{m}$, with nearly rectangular profiles, and large ratios of their depths to widths (aspect

ratios). Rectangular microchannels are completely defined by their width, depth and length, facilitating the calculation of flow through them and making microfluidic networks largely reproducible.

The single most expensive piece of equipment required for the rapid prototyping of microfluidic devices using UV lithography is a source of collimated UV light (UV flood source). A standard UV flood source is built around a powerful high-pressure mercury lamp and requires a matching power supply with a feedback loop for steady illumination. A UV flood source also usually has elements absorbing infrared (IR) and visible light (to reduce heating of the target), an electro-mechanical shutter to control the exposure, and UV-transparent optical elements to collimate and uniformly distribute light over a large target area. Even if the light source is only used sparsely, mercury lamps are often kept on continuously because of their long warm-up times and the adverse effect that restarting has on their longevity. As a result, in addition to the cost of replacement of the mercury lamps, the power costs alone can be as much as $\$1000$ a year.

The light produced by mercury lamps has a broad spectrum, including bright lines in deep UV, making them versatile sources of illumination for fluorescence microscopy and UV lithography. Nevertheless, deep UV light represents a problem for fabrication of tall reliefs of SU8, which are required for deep micro-channels in PDMS. The UV absorbance of SU8 sharply increases at wavelengths below 350 nm , and to obtain straight walls for relief features taller than $\sim 25 \text{ }\mu\text{m}$ the manufacturer recommends filtering those wavelengths out. Among additional problematic features of mercury light sources are fluctuations in the spatial distribution of illumination and continuous drift in the intensity of illumination.

High-power light-emitting diodes (LEDs) have been increasingly replacing mercury lamps in light sources used for fluorescence microscopy.¹⁻³ Whereas LEDs may still be inferior to high-pressure mercury lamps in terms of the maximal intensity of illumination, LEDs have multiple advantages, including narrow emission bands, stable illumination patterns with steady and reproducible light intensity, very short response times, and low power consumption. LEDs are even more appealing for light curing applications, where the light intensity is usually relatively low and a large area can be illuminated nearly uniformly by an array of evenly spaced LEDs with no additional optical elements involved. Affordable high-power LEDs are currently available with

wavelengths as short as 365 nm, and LED-based near-UV curing systems are now offered by multiple manufacturers.

Arrays of near-UV LEDs have also recently been used by several groups for contact lithography.^{4–6} These arrays were assembled from large numbers of low-power individual LEDs, which had relatively large divergence of light emanating from them (large viewing angles). Large divergence angles and the resulting overlapping of light from multiple individual LEDs can improve the spatial uniformity of illumination,^{4, 6} as required for UV curing and contact lithography with thin layers of photoresist. However, if applied to thick layers of SU8 to fabricate PDMS microfluidic devices with deep micro-channels (e.g., 100 μm or more), UV illumination with large divergence is expected to result in uneven exposure through the thickness of SU8, produce features with uneven width, and complicate the fabrication of features with large aspect ratios. Reductions in the divergence of light (improvement of its collimation) have been achieved by blocking the light emerging from the sides of LEDs in a large array.⁵ Nevertheless, the resulting illumination pattern was visibly uneven, bearing clear fingerprints of the locations and internal structure of individual LEDs. Nearly-uniform illumination has also been achieved with a single large-area LED.⁷ However, this LED had a full width at half-maximum (FWHM) viewing angle of $\sim 100^\circ$, making it difficult to combine uniformity of illumination with high intensity and low divergence.

A commercial mask aligner with a UV-light source based on LEDs that produces uniform and collimated illumination has recently become available (MDA-400LJ by MIDAS Systems, Daejeon, Korea). However, with a price tag of \$65,000, this mask aligner would be a considerable investment. Here we present a UV lithography light source (Fig. 1), which is based on a square array of nine high-power 365 nm LEDs, produces collimated and uniform illumination over a 3.5 inch square, and is built at a cost of <\$1000 in parts, materials, and machining. We demonstrate the utility of the UV-light source by performing photolithography with SU8 and two positive photoresists and by fabricating PDMS channels with near-rectangular profiles over a range of depths.

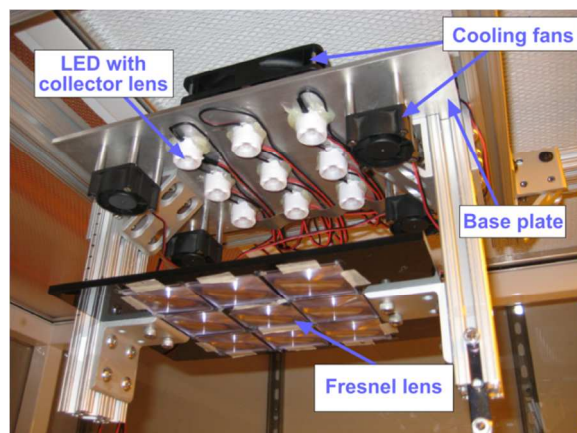


Figure 1. Photograph of the LED UV light source mounted to ceiling of clean room using 80/20 extrusions and brackets

Materials and Methods

The LEDs (LZ1-10U600 by LED Engin, San Jose, CA, with a nominal radiant power of 320 mW at a current of 0.7 A) are mounted on a 3/16" aluminum base plate in a 3x3 square array with a pitch of 50 mm. To prevent excessive heating of the LEDs, which dissipate $\sim 3\text{ W}$ each at a 0.7 A current, five fans with standoffs are mounted on the base plate, with four smaller fans on the same side as the LEDs and a larger fan on the back side. The divergence (viewing angle) of light coming from individual LEDs is reduced from $\sim 80^\circ$ to

$\sim 12^\circ$ FWHM by gluing a commercial light-collecting UV lens (FCN12592_LE1-D-COP, by LEDiL, Finland) to each LED (Fig. 1 and Supplementary Fig. S-1).

To further reduce the divergence, we use a 3x3 square array (with the same pitch of 50 mm) of nine identical converging polyvinylchloride (PVC) Fresnel lenses with a focal length $f \approx 180$ mm. The lenses are mounted on a black acrylic plate with 44 mm apertures and positioned at a distance of ~ 127 mm from the base plate (~ 124 mm and ~ 109 mm, respectively, from the emitting surfaces of the LEDs and the front surfaces of the collecting lenses; Supplementary Fig. S-1). The thin PVC lenses (#401B, <http://www.3dlens.com>) are chosen because of their low cost and high transparency at 365 nm. Placing a converging lens at a distance $L < f$ from a point source of light reduces the divergence of the beam from the source by a factor of $f/(f-L)$. With the front surface of a collecting lens taken as the new source of light, corresponding to $L = 109$ mm, this equation predicts the divergence to decrease from $\sim 12^\circ$ to $\sim 4.7^\circ$. However, because of the large thickness of the collecting lenses (~ 15 mm) and complex light paths in them, the value of $\sim 4.7^\circ$ can only be used as an estimate.

For the light source to illuminate the target evenly, the beams from adjacent LEDs must partially overlap.⁸ Given the relatively large distance between the individual LEDs and the low beam divergence, the light source in the proposed setup must be placed a sufficient distance from the target to achieve sufficient beam overlap. To this end, we use the simple practical solution of mounting the light source on the ceiling of our modular clean room. The distance from the base plate to the target (photomask holder) is 960 mm (Supplementary Fig. S-1). The mounting setup includes aluminum extrusions (rails), connecting plates, brackets, and corner gussets from 80/20 Inc. (Columbia City, IN), which are used to align the light source with the target area (photomask holder) and to adjust the distance between the Fresnel lens array and the LED array for optimal illumination.

The LED array is powered by a 40V, 2A digital power supply (by Lambda). Because the radiant power of an LED is primarily the function of the current, the power supply operates in current regulating mode and the LEDs are connected in series. To adjust the illumination, the currents through the four LEDs in the corners, four LEDs at the edges, and the LED in the center are tuned separately (Supplementary Fig. S-2). To this end, a potentiometer is connected in parallel with the five LEDs that are not in the corner positions, and another potentiometer is connected in parallel with the central LED. The exposure time is controlled with a multi-function time delay relay with mechanically adjustable intervals from 0.1 sec to 60 hrs (H3CR-A8 by Omron).

Results

The distance, L , and the currents through different groups of LEDs were adjusted to achieve high uniformity of illumination without substantially compromising its intensity or collimation (and it is as a result of this adjustment that L was set to 109 mm). The currents through the corner, edge, and central LEDs were set at 0.6, 0.3, and 0.15 A, respectively. Photographs of the UV illumination fields produced by individual LEDs (Supplementary Fig. S-3) and all LEDs together (Supplementary Fig. S-4) did not show appreciable variations of intensity at scales smaller than ~ 25 mm (half of the pitch of the LED array). Therefore, we measured the UV intensity distributions directly using a UV power meter (#0306-001-4 by OAI) with a 6.5 mm diameter optical window and a peak response at 365 nm. Illumination spots produced by individual LEDs had diameters (FWHM) of ~ 42 mm at the target and ~ 30 mm at 250 mm above it, corresponding to a divergence angle of 5.4° , in reasonable agreement with the theoretical estimate of 4.7° .

To obtain a detailed map of the illumination field, we divided a 120×120 mm area around the center into a 12×12 array of 10 mm squares and measured the UV intensity in the middle of each square with the power meter. The results (Fig. 2) indicated that in the central 90×90 mm target area (square photomask used with a 5 in. wafer), the intensity had a mean value of 1.75 mW/cm² with an SD of 0.05 mW/cm², corresponding to a coefficient of variation (CV) of 2.9%. The peak-to-peak variation of the intensity was 0.26 mW/cm², corresponding to 15% of the mean. With the four squares at the corners of the 90×90 mm target area excluded, the peak-to-peak variation dropped to 11% of the mean.

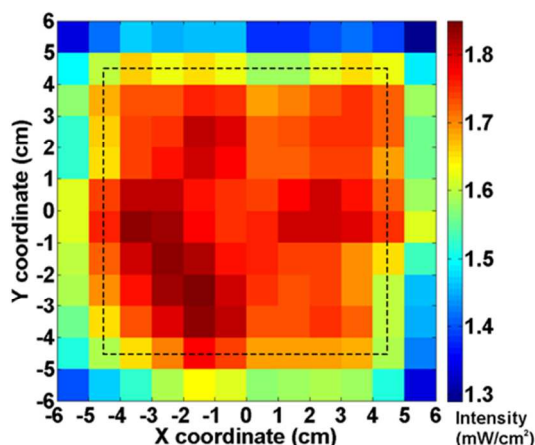


Figure 2. Color-coded plot of the UV intensity in a 12×12 cm region centered at the 9×9 cm target area (delineated by the dashed black square), as measured in the centers of 1×1 cm squares with a UV power meter with peak sensitivity at 365 nm. (Note that the lowest intensity is 1.3 mW/cm² rather than 0.)

To test the utility of the UV light source for fabrication of microfluidic devices in PDMS, we used a photomask with a 5×5 array of 18 mm squares with identical test patterns, each having 4 identical clusters (for testing 4 different exposure times) of transparent strips with widths from ~23 to ~160 μm and separations from ~17 to ~78 μm. (After passing through a transparent area of the photomask mounted on a 0.080" glass support, the UV light intensity decreased by ~22%.) The photomask was used with three 5 in. wafers, which were spin-coated with 25±1 μm, 160±28 μm, and 311±11 μm (mean±SD) thick layers of the SU8 photoresist. After the wafers were exposed to UV through the photomask, post-baked, and developed (Fig. 3a and Supplementary Fig. S-5), a PDMS (Sylgard 184 by Dow Corning) replicas were made and cut into 25 square chips, corresponding to the 25 copies of the test pattern on the photomask (Fig. 3b). Each chip was then sliced in the vertical plane perpendicularly to the microchannels, which were the replicas of the SU8 ridges produced by the transparent strips on the photomask. The cross-sections of the microchannels were photographed under a darkfield microscope (Fig. 3c).

For the 311 μm SU8 layer, exposure times of 4, 6, 8, and 10 min were tested. Best results were obtained with the 6 min exposure (Supplementary Fig. S-5), corresponding to a cumulative irradiation of ~490 mJ/cm². Specifically, in all 25 test areas, arrays of 82 μm wide transparent strips with 78 μm separations produced arrays of well-separated channels (Fig. 3c). The cross-sections of individual channels in different test areas were analyzed by digitally processing their micrographs using a code in MatLab to obtain the channel widths at different distances from the surface of the PDMS chips (excluding most proximal and most distal 10 μm) (Fig. 4). (The digital processing procedure is described in Supplementary Information.) The peak-to-peak variations of widths of individual

channels in different test areas ranged from 4.46 μm to 14.0 μm, with the SD ranging from 1.2 μm to 4.3 μm (Fig. 4). When normalized to the average channel depth of 311 μm, these numbers corresponded to a peak-to-peak variability of 1.4% to 4.5% and CV of 0.4% to 1.4% (Supplementary Table S-1). Importantly, channel width at the positions most proximal and most distal to the surface of PDMS, corresponding to "bottoms" and "tops" of the SU8 ridges on the wafer, differed by <4.2 μm on average (CV<1.3%), suggesting that the channel cross-sections were near-rectangular, as expected for uniform and collimated UV irradiation of the SU8 photoresist. The average widths of the channels in the 25 test regions varied from 92 μm to 102 μm with a mean of 96 μm and an SD of 2.4 μm, corresponding to SV of 0.75% (when normalized to the channel depth again).

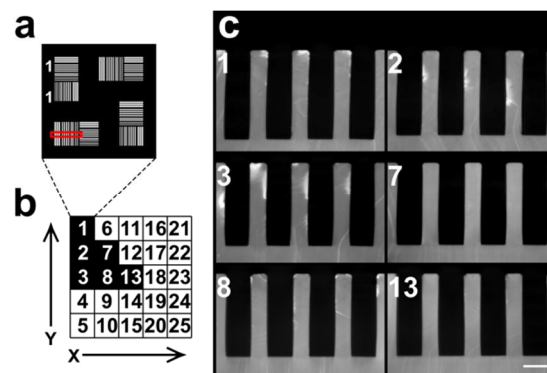


Figure 3. PDMS chips with 311 μm deep microchannels fabricated using a test photomask. (a) Fragment of the photomask showing one 18×18 mm test pattern from the 5×5 array of identical test patterns. Each test pattern has four identical clusters of transparent strips, which include four strips each: 23 μm wide with 17 μm separations, 41 μm wide with 39 μm separations, 82 μm wide with 78 μm separations, 160 μm wide strips 80 μm separations, four 163 μm wide with 157 μm separations. The red rectangle marks an area of the PDMS chip made with the photomask that is cut and examined under a darkfield microscope. (b) A map with continuous enumeration of the test patterns in the 5×5 array. (c) Micrographs of cross-sections of microchannels in PDMS chips cast from 6 representative regions of the wafer with different locations within the 5×5 test pattern array, as indicated by numbers, corresponding to the highlighted squares in panel b. The microchannels are replicas from relief features produced by a 6 min exposure of a 311 μm thick (on average) SU8 layer through 82 μm wide transparent strips with 78 μm separations. The micrographs are taken with a 10x objective under darkfield illumination. Scale bar 100 μm.

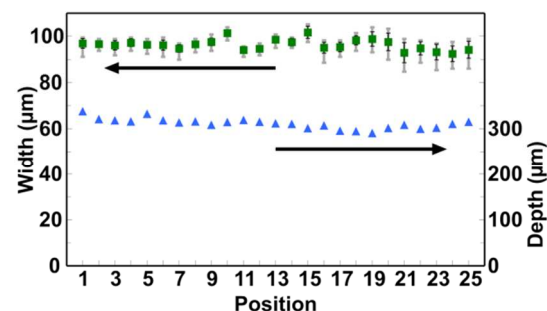


Figure 4. The width of a microchannel averaged over its depth (green squares) and microchannel depth (blue triangles) for each position within the 5×5 test pattern array. All microchannels are replicas of ridges produced by a 6 min UV exposure of a 311 μm thick (on average) layer of SU8 through 82 μm transparent strips.

Black error bars show standard deviations of the widths; grey error bars show ranges of widths measured.

We note that, whereas there is an appreciable difference between the mean width of the channels and the width of the transparent strips on the photomask, this difference can be accounted for in the design of the photomasks. The differences between the cross-sections of nearby channels in the arrays of four (cf. Fig. 3c) were smaller than but comparable to the differences between channels from different test areas (Supplementary Information and Fig. S-6). The mean widths of the channels and partitions ($\sim 64\ \mu\text{m}$) correspond to aspect ratios (depth/width) of ~ 3 and ~ 5 , respectively, which are both relatively high for microchannels cast in PDMS. The 4 min exposure resulted in a closer matching between the mean width of the microchannels and the width of the transparent strips on the photomask (89 vs. $82\ \mu\text{m}$) at expense of reduced uniformity of the channel widths (Supplementary Fig. S-7).

For the 160 and $25\ \mu\text{m}$ SU8 layers, the optimal exposure times were 4 and 3 min, respectively (Supplementary Fig. S-8 and S-9). The widths of the microchannels matched the widths of the transparent strips more closely, $92\ \text{vs.}\ 82\ \mu\text{m}$ for the $160\ \mu\text{m}$ layer and $26\ \text{vs.}\ 23\ \mu\text{m}$ for the $25\ \mu\text{m}$ layer (Supplementary Table S-1). The average values of CV of the channel width were 0.9 and 2.9% for the 160 and $25\ \mu\text{m}$ layers, respectively, and partitions between channels had mean aspect ratios of ~ 2.4 and ~ 1.8 , respectively.

The UV light source was also successfully used to produce SU8 reliefs as thick as $1\ \text{mm}$ (Supplementary Fig. S-10) and as thin as $\sim 0.5\ \mu\text{m}$ (Supplementary Fig. S-11). In the latter case, the photolithography was done using a high-resolution chrome mask with a periodic pattern of $1.5\ \mu\text{m}$ transparent strips and $1.5\ \mu\text{m}$ reflective partitions that was transferred onto the SU8 photoresist with a high fidelity (Supplementary Fig. S-11). Finally, we tested the UV light source with two positive photoresists sensitive to 365 nm UV (i-line), SPR 220-7.0 (by Dow Chemical Company) and AZ40XT-11D (by AZ Electronic materials). The photoresists were spin-coated onto 5 inch wafers to thicknesses of ~ 8 and $\sim 30\ \mu\text{m}$, respectively. We used the same photomask as with the 25, 160, and $311\ \mu\text{m}$ layers of SU8 (Fig. 3), and its test pattern of transparent and opaque strips of different widths was successfully transferred onto both photoresists (Supplementary Fig. S12).

Discussion and Conclusions

The proposed LED-based UV light source is an effective tool for SU8 photolithography aimed at the fabrication of rectangular microchannels in PDMS with a variety of depths. The UV light source also enables photolithography with positive photoresists sensitive to 365 nm UV (i-line). The UV light source provides collimated uniform illumination over a large area, making it possible to fabricate microchannels with consistent widths and high aspect ratios. Unlike a mercury lamp UV light source, neither the spatial pattern nor light intensity of the LED light source changes with time, eliminating the need to periodically calibrate the illumination and modify the fabrication protocols.

The narrow spectrum of the LEDs, which is centered at 365 nm, corresponding to a characteristic SU8 absorption length of $\sim 370\ \mu\text{m}$,⁹ leads to a relatively weak dependence of the optimal exposure time on the thickness of SU8 layer, making the fabrication more forgiving. So, in our tests, good quality reliefs of SU8 with thicknesses from 25 to $311\ \mu\text{m}$ (and good-quality PDMS microchannels with the corresponding depths) were produced using a single exposure time of 4 min, corresponding to $\sim 330\ \text{mJ/cm}^2$ cumulative irradiation. Furthermore, we noticed that thick ($>200\ \mu\text{m}$) SU8 patterns were more robust and strongly adherent to the wafers when made with the LED source rather than a 350 W

mercury lamp UV flood source equipped with a colored-glass long-pass filter (Schott WG-360, with 50% absorption at 360 nm). We explain this increased robustness and adhesion by the narrower spectrum of the LEDs with no deep UV light in it, leading to greater uniformity of the exposure over the SU8 depth. As of now, our lab has completely switched to using the LED-based UV source for SU8 photolithography and stopped using the mercury lamp source (made by OAI and priced at $\sim \$15,000$ in 2002) that we have been using during the last 11 years.

The LED-based UV light source costs $< \$1000$ in parts, materials, and machining to build, and because the LEDs are only powered during the UV exposures and are expected to last ~ 5000 hrs (50,000 exposures of 6 min), its maintenance costs are close to zero. The intensity of the illumination can be substantially increased and the exposure times can be proportionally reduced using recently introduced 365 nm LEDs (LZ1-00UV00 by LED Engin), which are ~ 2.5 times more luminous than the LEDs used in our source. In addition, the collimation and uniformity of illumination can likely be further improved by customizing the geometry of the LED array (e.g., using a triangular array with a different pitch)⁸ and increasing the number of LEDs in the array. The low costs of manufacture and maintenance of the light source make it particularly appealing for microfluidic teaching laboratories, microfluidic research and development laboratories, and small academic and industrial fabrication facilities in general.

Acknowledgements

We thank Philibert Tsai for illuminating discussions. The work was partially funded by NSF PHY 1205921 and NSF PHY 0750049 awards.

Notes and references

^a Department of Physics, University of California, San Diego, 9500 Gilman Drive, MC 0374, La Jolla, CA, 92093, USA

*e-mail: agroisman@ucsd.edu

† Electronic Supplementary Information (ESI) available: [details of any supplementary information available should be included here]. See DOI: 10.1039/c000000x/

1. P. Herman, B. P. Maliwal, H.-J. Lin and J. R. Lakowicz, *Journal of Microscopy*, 2001, **203**, 176-181.
2. I. T. Young, Y. Garini, H. R. C. Dietrich, W. van Oel and G. L. Lung, LEDs for fluorescence microscopy, 2004.
3. H. R. Petty, *Microscopy research and technique*, 2007, **70**, 687-709.
4. M. D. Huntington and T. W. Odom, *Small*, 2011, **7**, 3144.
5. J. Kim, S. Paik, F. Herrault and M. G. Allen, presented in part at the Proc. Solid-State Sensors and Actuators Workshop, Hilton Head, June, 2012.
6. M. K. Yapici and I. Farhat, *Optical Microlithography Xxvii*, 2014, **9052**.
7. M. C. Breadmore and R. M. Guijt, *Journal of Chromatography A*, 2008, **1213**, 3.
8. I. Moreno, M. Avendaño-Alejo and R. I. Tzonchev, *Applied Optics*, 2006, **45**, 2265.
9. E. F. Reznikova, J. Mohr and H. Hein, *Microsystem technologies*, 2005, **11**, 282-291.